Neurotox Res (2017) 32:671–682
DOI 10.1007/s12640-017-9785-y

ORIGINAL ARTICLE

Effects of Hydroxyurea Exposure on the Rat Cerebellar Neuroepithelium: an Immunohistochemical and Electron Microscopic Study Along the Anteroposterior and Mediolateral Axes

Lucía Rodríguez-Vázquez[1] · **Joaquín Martí**[1]

Received: 30 May 2017 / Revised: 11 July 2017 / Accepted: 12 July 2017 / Published online: 25 July 2017

Abstract We present a histological study of the cell death of cerebellar neuroepithelial neuroblasts following treatment with the cytotoxic agent hydroxyurea (HU) during the embryonic life. Pregnant rats were treated with a single dose of HU (300 mg/kg) at embryonic days 13, 14, or 15 of gestation, and their fetuses were studied from 5 to 35 h after treatment to elucidate the mechanisms of HU-induced fetotoxicity. Quantification of several parameters such as the density of pyknotic, mitotic, and PCNA-immunoreactive cells indicated that HU compromises the survival of the cerebellar neuroepithelium neuroblasts. On the other hand, our light and electron microscopic investigations during the course of prenatal development indicated that HU leads to two types of cell death: apoptosis and cells presenting cytoplasmic vacuolization, altered organelles, and a recognizable cell nucleus. Both modalities of cell death resulted in a substantial loss of cerebellar neuroepithelium cells. Current results suggest that HU exposure during gestation is toxic to the cerebellar neuroepithelium. Moreover, they allow to examine the mechanisms of HU-induced toxicity during the early development of the central nervous system. Our data also suggest that it is essential to avoid underestimating the adverse effects of HU when administered during early prenatal life.

Keywords Prenatal · Hydroxyurea · Cerebellar neuroepithelium · Apoptosis · Electron microscopy

✉ Joaquín Martí
joaquim.marti.clua@uab.es

[1] Unidad de Citología e Histología, Facultad de Biociencias, Universidad Autónoma de Barcelona, 08193 Bellaterra, Barcelona, Spain

Introduction

The cerebellum presents a regular cytoarchitecture. It is composed of a limited number of neurons, which are specifically integrated in the corticonuclear network and are characterized by a distinctive morphology and molecular markers (Schilling et al. 2008; Haines and Dietrichs 2012). Several studies have indicated that the isthmic organizer, located at the mesencephalon/rhombomere 1 boundary, directs the formation of the cerebellar territory (Martinez et al. 2013). The establishment of the cerebellar territory is followed by the formation of two germinative compartments: the rhombic lip and the ventricular neuroepithelium (Yaguchi et al. 2009; Tong et al. 2015).

All cerebellar neurons originate from the abovementioned regions according to a well-defined spatiotemporal sequence (Sillitoe and Joyner 2007; Leto et al. 2016). Glutaminergic cells, including unipolar brush cells, granule cells, and some projection deep cerebellar nuclei (DCN) neurons, arise from the rostral rhombic lip and undergo subsequent waves of differentiation (Leto et al. 2012). GABAergic neurons, on the other hand, originate from the ventricular neuroepithelium (Grimaldi et al. 2009; Leto et al. 2009). Purkinje cells (PCs), inhibitory interneurons, DCN neurons, and nucleo-olivary neurons are specified within this germinal site at the onset of the cerebellar neurogenesis (Marzban et al. 2015).

Hydroxyurea (HU) or hydroxycarbamide is a non-alkylating agent (chemical formula $CH_4N_2O_2$) (Navarra and Preziosi 1999). This chemical compound is used for the treatment of neoplasms (Saban and Bujak 2009). The clinical use of HU as an anticancer agent is based on the drug's ability to reduce the production of deoxyribonucleotides that are necessary for DNA replication. This occurs via inhibition of the class I form of ribonucleotide reductase by inactivating the tyrosyl radical required for enzyme activity, without interfering with the synthesis of ribonucleic acids or proteins (Shao

et al. 2006; Saban and Bujak 2009). HU has been also used for a variety of conditions in the disciplines of hematology (Navarra and Preziosi 1999; Ware et al. 2011; Nevitt et al. 2017), infectious disease (Zala et al. 2000), and dermatology (Lebwohl et al. 2004).

There are many reports of HU-related detrimental effects. When administered to pregnant dams, it compromises the ability of embryos to develop (Sampson et al. 2010) and induces in them alterations in the craniofacial tissues (Schlisser and Hales 2013), growth retardation, and loss of mesenchymal cells in the lung (Woo et al. 2004; Woo et al. 2005). HU also produces microencephaly, hydrocephalus, and apoptosis in neuroepithelial cells (Woo et al. 2003, 2004, 2006).

Previous studies from our laboratory have indicated that when administered in the early postnatal life, the cytotoxic agent HU leads to the activation of apoptotic cellular events in the cerebellar external granular layer as well as to alterations in the cerebellar cortex cytoarchitecture (Martí et al. 2017). Moreover, our results have also indicated that HU reduces the number of PCs and DCN neurons. It also alters the neurogenetic timetables and the neurogenetic gradients of these macroneurons in rats that were exposed to this agent as embryos and then assessed at 90 days of age (Martí et al. 2016).

In light of the above, we began a set of experiments in our laboratory. The major goal of this article is to study the effect of HU treatment on the development of the rat cerebellar neuroepithelium in the prenatal life. Three ages were studied: embryonic days (E) 13, 14, and 15. These ages were selected because in normal rats, the neurogenetic timetables of PCs and DCN neurons extend from E13 to E15 (Altman and Bayer 1997; Martí et al. 2015, 2016). The selection of the cerebellum was supported by the evidence that this is an organ particularly amenable to the analysis of pattern formation because of its highly organized structure (Butts et al. 2014; Marzban et al. 2015). Additionally, the cerebellum is highly vulnerable to intoxication (Manto 2012; Samson and Claassen 2017).

In particular, the following aspects were addressed: (I) we characterized the effect of HU exposure on the cerebellar neuroepithelial cells. This was carried out by quantifying the density of pyknotic, mitotic, and proliferating cell nuclear antigen (PCNA)-positive cells after a single dose of HU, and (II) we used terminal deoxynucleotidyl transferase dUTP nick-end labeling (TUNEL) and transmission electron microscopy to study cell degeneration in the cerebellar neuroepithelium following HU exposure.

Materials and Methods

Animals

All experiments in this study were carried out in accordance with the requirements of the Committee for Institutional Animal Care and Use in the Universitat Autònoma de Barcelona (UAB). The number of animals was kept to a minimum, and all efforts were made to minimize their suffering. Timed-pregnant Sprague Dawley OFA rats were obtained from the animal production facility at the UAB. Dams were administered intraperitoneally at 8:30 a.m. with a single injection of saline (0.9% NaCl) or HU (Sigma, St. Louis, MO, USA) (300 mg/kg b.w.) according to the following time-windows: E13, E14, and E15.

Embryos were sacrificed at regular intervals from 5 to 35 h after HU exposure. In each time-window, 70 pregnant dams were used; 35 were injected with saline and 35 with HU (300 mg/kg). From each dam, two embryos were analyzed. As an example, schedules for E13 are listed in Table 1. E1 was deemed to be the morning after mating. During the experimental procedures, rats were maintained under standard laboratory conditions (temperature of 22 ± 2 °C and relative humidity of 55 ± 5%, 12 h light-dark cycle starting at 08:00 a.m., food and water were provided ad libitum).

Tissue Processing

Dams were weighed and anesthetized with a ketamine-xylazine mixture (90:10 mg/ml; 1 ml/kg, intraperitoneal). Embryos were removed by caesarian, and their heads were immediately immersed in 10% neutral buffered formalin for 24 h at 4 °C. These were paraffin-embedded and sectioned at 10 μm in the sagittal and coronal planes. The levels used for analysis correspond to the plates of figures from Altman and Bayer (1995). These are indicated in Table 2. As the cerebellar neuroepithelium, interphase nuclei, and mitotic figure's diameter in the area of reference are larger than the slice thickness, only one in every five sections was placed on poly-(L-lysine)-coated slide in order to avoid overestimation of cell counts.

Feulgen Method

Feulgen staining was performed according to previously published procedures (Hervás et al. 2002; Marti et al. 2016). Sections were deparaffinized in xylene and rehydrated through a series of graded ethanol. Partial denaturation of DNA was carried out with 3 N HCl at 40 °C for 15 min. Hydrolysis was halted by two washes in distilled water at RT, and then the sections were treated 1 h in darkness with Schiff's reagent (prepared from basic fuchsin; Fluka Chemie, Buchs, Switzerland) at RT. After washing in fresh sulfurous acid solution, the stained sections were rinsed in distilled water, dehydrated, and coverslipped.

TUNEL Staining

TUNEL staining was done with an in situ cell death detection kit (POD Roche Diagnostics, cat. 11684817910). In brief, after

Table 1 Schedules of saline and hydroxyurea administrations and sacrifice at embryonic day 13

Treatment	Sacrifice (hours)						
E12	5	10	15	20	25	30	35
Saline [5]	S						
Saline [5]		S					
Saline [5]			S				
Saline [5]				S			
Saline [5]					S		
Saline [5]						S	
Saline [5]							S
HU [5] (300 mg/kg)	S						
HU [5] (300 mg/kg)		S					
HU [5] (300 mg/kg)			S				
HU [5] (300 mg/kg)				S			
HU [5] (300 mg/kg)					S		
HU [5] (300 mg/kg)						S	
HU [5] (300 mg/kg)							S

Values in brackets represent the number of dams used

E embryonic day, *S* sacrifice, *HU* hydroxyurea

removing paraffin, sections were incubated with proteinase K, nuclease free (20 μg/ml in 10 mM Tris-HCl, pH 7.5) during 30 min at room temperature. They were then cleaned with PBS and incubated for 10 min with 3% H_2O_2 in methanol. Slices were soaked in the TUNEL reaction mixture for 60 min at 37 °C and then cleaned with PBS. Subsequently, sections were incubated with converted POD for 30 min at 37 °C. After further rinsing in PBS, the peroxidase coloring reaction was developed by 3,3′-diaminobenzidine-H_2O_2 for 5 min, and sections were then rinsed in distilled water and counterstained with hematoxylin. For positive control of TUNEL labeling, histological sections were incubated with DNase (5 μg/ml) at 37 °C during 10 min to induce DNA strand breaks.

PCNA Immunocytochemistry

Sections were deparaffinized following regular procedures from our laboratory. These were immersed in Coplin jars containing15 mM of heated (96–99 °C) sodium citrate buffer (pH 6.0) and incubated in the water bath containing water at 96–99 °C for 20 min. After that, the slices were allowed to cool for 20 min. The endogenous peroxidase activity was blocked with 3% H_2O_2 for 10 min at room temperature. Non-binding sites were blocked using 5% bovine serum albumin in PBS containing 0.1% Tween-20 and 5% normal goat serum for 1 h at room temperature. Following this, the slides were incubated at room temperature with monoclonal mouse anti-mouse anti-PCNA (1:1500, Santa Cruz Biotechnology, clone: PC-10, Catalog number: sc-56). After this, sections were rinsed with PBS and incubated at room temperature for 30 min with a biotin conjugated goat anti-mouse IgG antibody (Sigma) 1:50 for 30 min and then exposed to ExtrAvidin-Peroxidase (Sigma) 1:50 for 30 min. Peroxidase activity was developed with 3,3′-diaminobenzidine-H_2O_2 (DAB, Sigma) for 5 min, and sections were then rinsed in distilled water. Control sections were prepared by replacing the primary antibody with PBS. These routinely showed no immunolabeling.

Quantitative Analyses

Counting of pyknotic cells, mitotic profiles, TUNEL, and PCNA-positive cells was carried out, at 63× oil immersion

Table 2 Levels used for quantitative analysis

Age	Sagittal plane		Coronal plane	
	Plate	Altman and Bayer book page	Plate	Altman and Bayer book page
	1	99	11	133
	2	101	12	135
E13	3	103	13	137
	4	105	14	139
	1	153	12	191
	2	155	13	193
E14	3	157	14	195
	4	159	15	197
	1	207	14	249
	2	209	15	251
E15	3	211	16	253
	4	213	17	255

The levels used for quantitative analysis are those indicated in Altman and Bayer atlas (Altman and Bayer 1995)

E embryonic day

objective, in the pertinent sections by visual scanning of the cerebellar neuroepithelium throughout its lateromedial and rostrocaudal axes. In embryos sectioned in the coronal plane, only the right cerebellar primordium was analyzed. Criteria for scoring pyknotic and mitotic cells included both morphological and staining properties with the reaction of Schiff. TUNEL and PCNA-positive cells were defined as those that have a brown reaction product over their nuclei.

The density of pyknotic, mitotic, TUNEL, and PCNA-stained cells was calculated as the percentage of the respective cell type over the area of the cerebellar neuroepithelium. The area of this parameter was determined using the ImageJ software (v. 1.43 u, NIH, Bethesda, MD, USA).

Transmission Electron Microscopy

For electron microscopy, the heads of the embryos were immersed in 2% glutaraldehyde and 2% paraformaldehyde in 0.1 M cacodylate buffer, pH 7.2. Tissue cubes (~1 mm^3) were rinsed in PBS, postfixed in 1% OsO_4 for 2 h, dehydrated in a graded ethanol series, infiltrated with propylene oxide, and embedded in Epon. Ultrathin sections (60 nm) were generated with an ultramicrotome (Leica AG, Reichert Ultracut S) and then viewed with a transmission electron microscope (JEM-1400). Digital images were obtained with a CCD GATAN 794 MSC 600HP digital camera system and analyzed using Adobe Photoshop software.

Data Analysis

The statistical significance of the results was evaluated with Student's *t* test or Mann-Whitney *U* test. When more than two means were simultaneously compared, one-way ANOVA followed by individual comparison of means with the Student-Newman-Keuls (SNK) test was used.

Photographic Material

The pictures presented in this report were captured with a color CCD-IRIS (Sony, Japan) video camera coupled to a Zeiss Axiophot microscope. The digitized images were processed in the Adobe Photoshop software.

Results

Studying the Cerebellar Primordium

The examination of cerebellar development in sagittally and coronally sectioned embryos showed that, for all of the studied time-windows (from E13 to E15), there were no alterations in the cytoarchitecture of the hindbrain of rats exposed to HU. Figure 1 shows representative sagittal (Fig. 1a–d) and coronal (Fig. 1e–h) sections of the hindbrain of E13 rats administered with saline. Embryos of this age present a cerebellar neuroepithelium composed of darkly stained and densely packed cells. When the cerebellar development was studied in sagittally sectioned embryos, it was observed that, caudally to the cerebellar primordium, the neuroepithelium was absent and was replaced by a membranous cover of the fourth ventricle, the medullary velum.

In coronal sections, on the other hand, the posterior boundary of the cerebellar neuroepithelium is defined by the medullary velum. The anterior one, however, deserves attention. This is because the cerebellar primordium is continuous with the isthmus during the early phases of

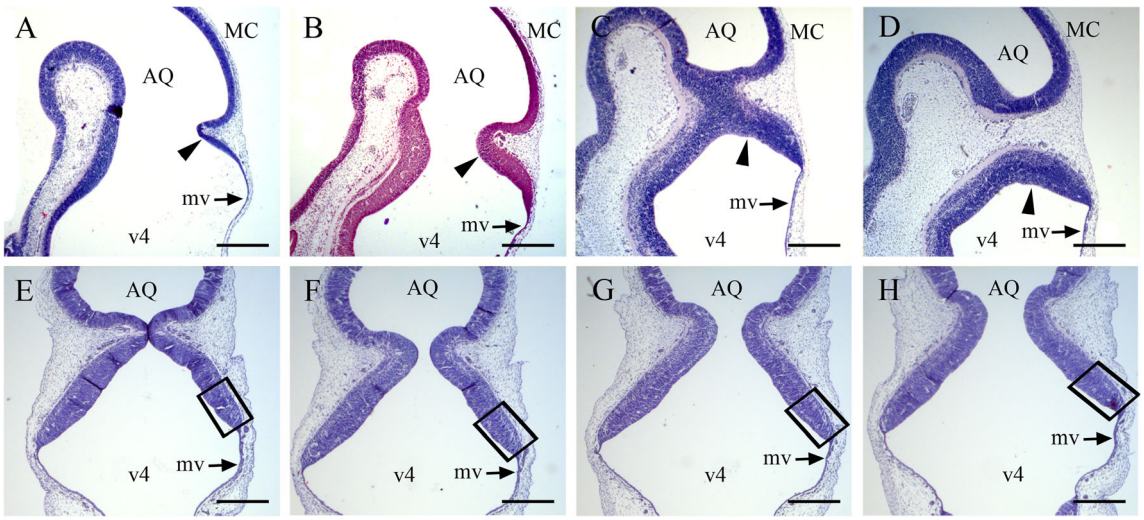

Fig. 1 Sagittal (**a**–**d**) and coronal (**e**–**h**) low-power photomicrographs of two rats sacrificed at embryonic day 14. *Arrowheads* in **a**–**d** outline the rostral boundary of the cerebellar primordium. The caudal one is traced by the medullary velum. In coronal sections, the posterior limit of the cerebellar primordium is delineated by the medullary velum. *Rectangles* mark the anterior boundary. *AQ* aqueduct; *MC* mesencephalon; *mv* medullary velum; *v4* fourth ventricle. *Scale bar*: 400 μm

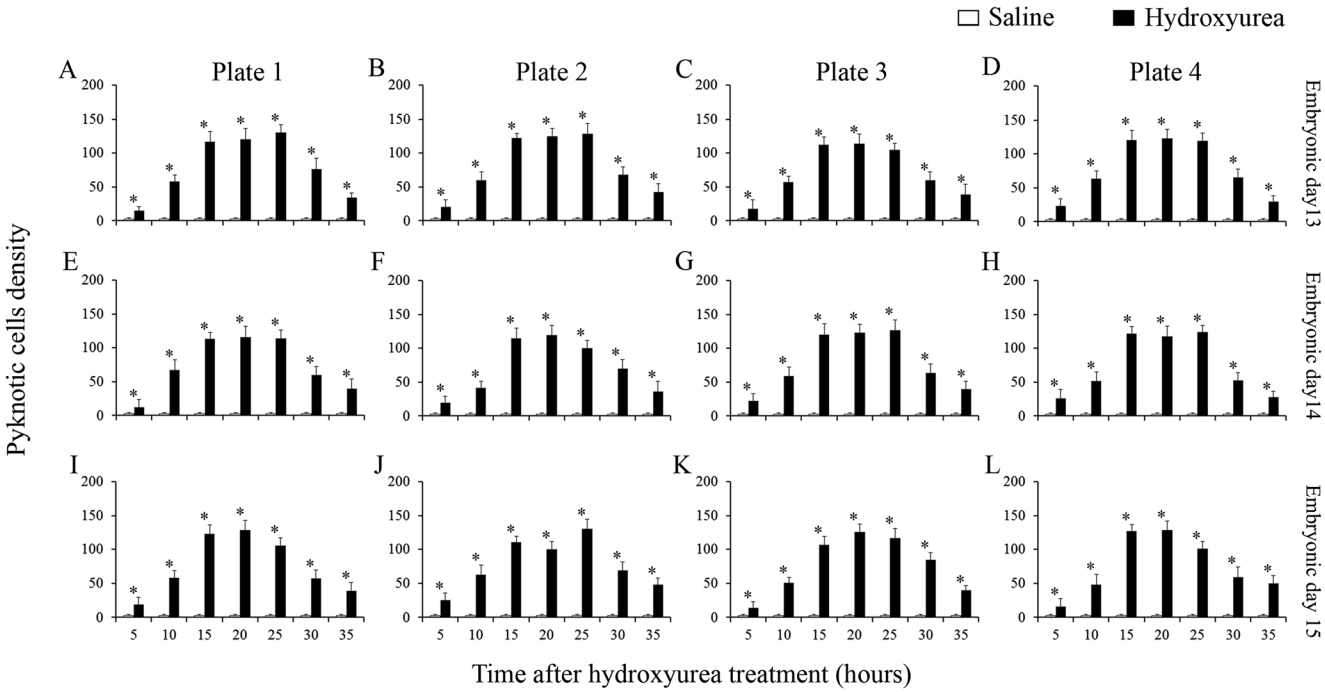

Fig. 2 Mean ± SEM for pyknotic cell density in the mediolateral axis of the cerebellar neuroepithelium [plates 1 to 4 from Altman and Bayer atlas, Altman and Bayer (1995)] are presented. Rats were injected with saline (*white columns*) or hydroxyurea (*black columns*) at embryonic days 13 to 15 and sacrificed several hours after treatment. *Significant at $P < 0.05$

embryonic development. Rectangles in Fig. 1e–h mark the anterior boundary. This delineation seems to be correct because, in line with previous reports (Altman and Bayer 1985, 1997), the right and left cerebellar primordia remain widely separated from each other from E13 to E15. In contrast, the isthmus has an unfused posterior part and a fused anterior part region that is continuous with the mesencephalon.

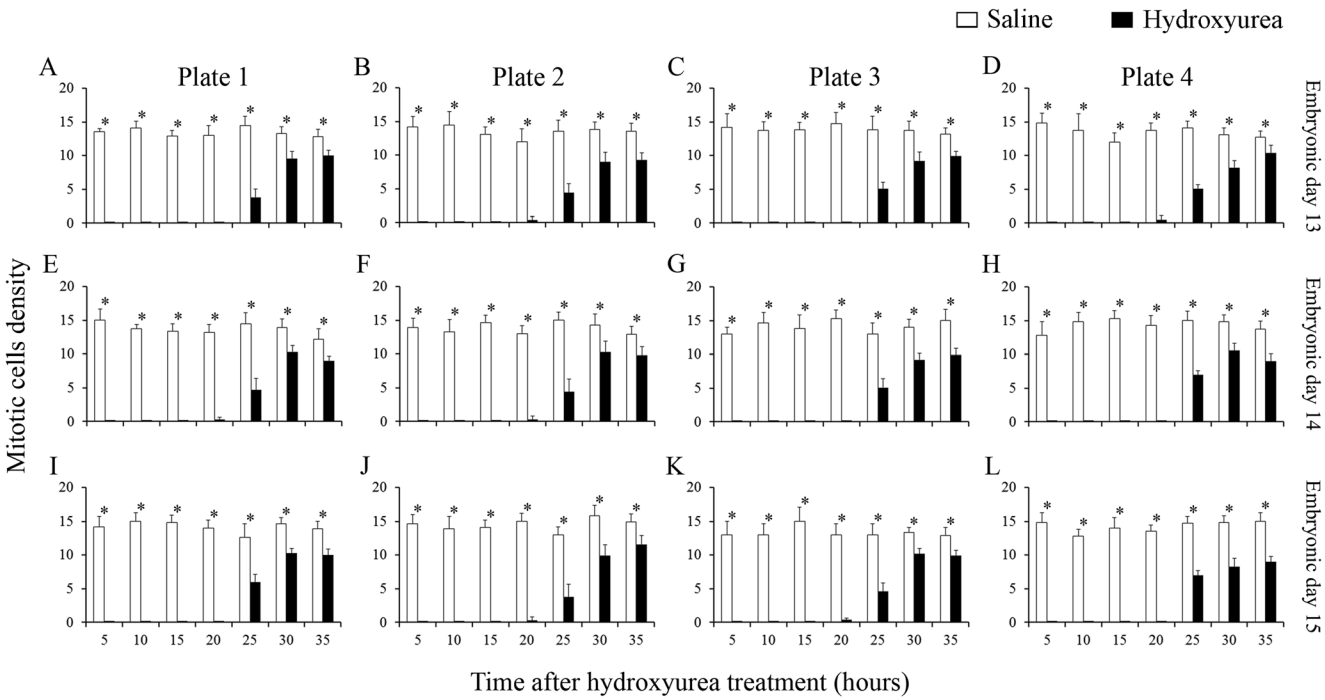

Fig. 3 Mean ± SEM for mitotic cell density in the mediolateral axis of the cerebellar neuroepithelium [plates 1 to 4 from Altman and Bayer atlas, Altman and Bayer (1995)] are presented. Rats were injected with saline (*white columns*) or hydroxyurea (*black columns*) at embryonic days 13 to 15. They were sacrificed several hours after treatment. *Significant at $P < 0.05$

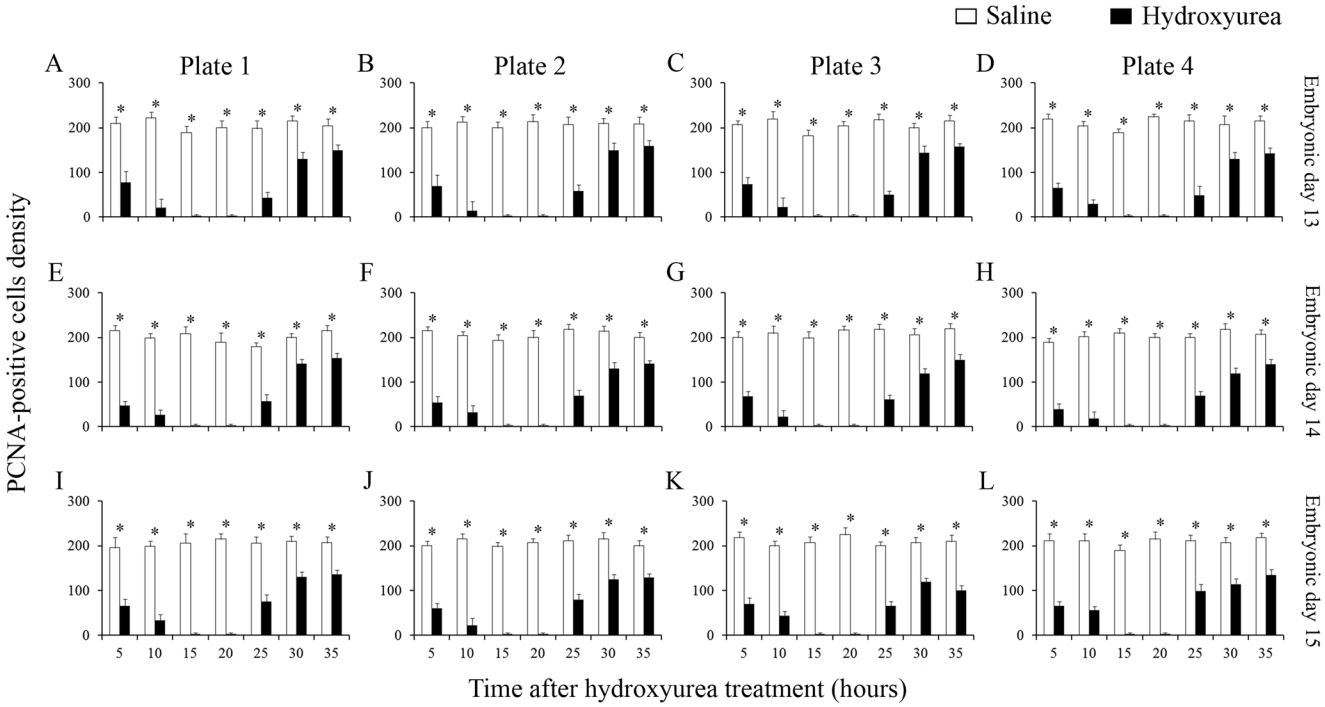

Fig. 4 Mean ± SEM for PCNA-positive cell density in the mediolateral axis of the cerebellar neuroepithelium [plates 1 to 4 from Altman and Bayer atlas, Altman and Bayer (1995)] are presented. Rats were injected with saline (*white columns*) or hydroxyurea (*black columns*) at embryonic days 13 to 15 and sacrificed several hours after treatment. *Significant at $P < 0.05$

Experiment 1

At the onset of the cerebellar development, the neuroepithelium contains cell precursors engaged in DNA synthesis. Cell depletion may be induced by toxic agents, which disrupt the proliferative dynamics of neuroblasts. This experiment was carried out to study the effect of HU exposure, an agent that inhibits DNA synthesis (Saban and Bujak 2009) on cerebellar neuroepithelial cells. This was done by quantifying, separately throughout the lateromedial and rostrocaudal axes, the density of pyknotic, mitotic, and PCNA-reactive cells per area of the cerebellar neuroepithelium.

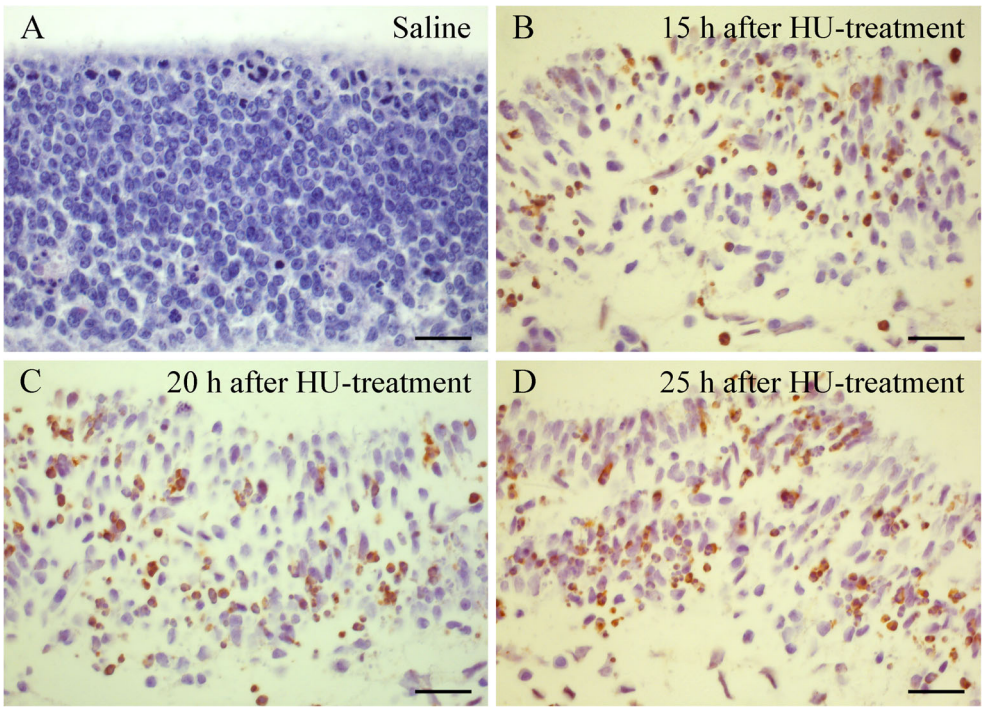

Fig. 5 Microscopic detection of TUNEL-positive cerebellar neuroepithelial cells in the mediolateral axis [plate 2 from Altman and Bayer atlas, Altman and Bayer (1995)]. Rats were treated with saline or hydroxyurea at embryonic day 14 and sacrificed at regular intervals after drug administration. TUNEL-positive cells are those presenting a brown reaction product in their nuclei. **a** Very few TUNEL-reactive cells are observed in the cerebellar neuroepithelium of saline rats. Massive cell death is found following 15 (**b**), 20 (**c**), and 25 h (**d**) of treatment. *Scale bar* 30 μm

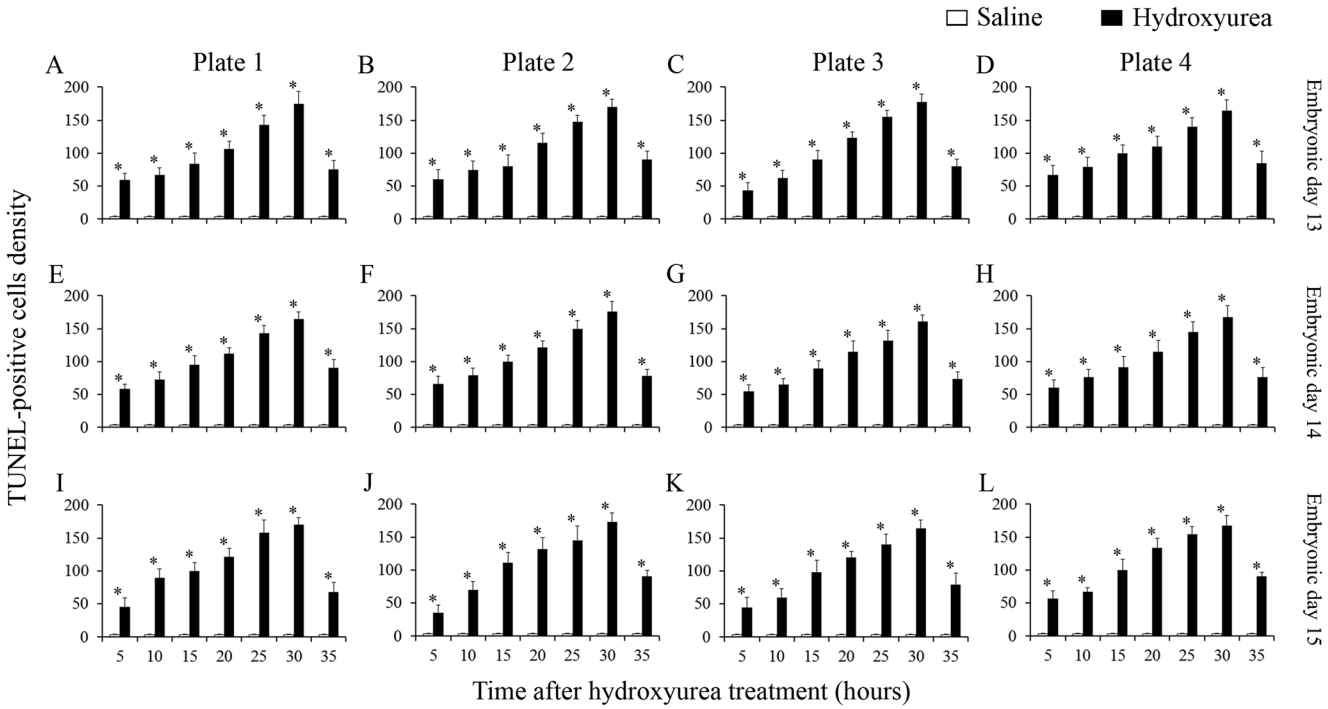

Fig. 6 Mean ± SEM for TUNEL-positive cell density in the mediolateral axis of the cerebellar neuroepithelium [plates 1 to 4 from Altman and Bayer atlas, Altman and Bayer (1995)] are presented. Rats were injected with saline (*white columns*) or hydroxyurea (*black columns*) at embryonic days 13 to 15 and sacrificed several hours after treatment. *Significant at $P < 0.05$

Regarding the mediolateral axis, the data of the measured parameters, in addition to the statistical analysis of the former parameters, are depicted in Figs. 2, 3, and 4. Current results indicated that, in all of the studied sagittal plates (1 to 4) and time-windows (from E13 to E15), the density of pyknotic cells began to increase 5 h after HU exposure, peaked at 20 h, and decreased thereafter (Fig. 2). On the other hand, no mitotic cells were observed until 25 h after drug administration. After such time, the density of this parameter increased, but it did not achieve saline values (Fig. 3). When the density of PCNA-positive cells was considered, values decreased in animals sacrificed 5 and 10 h after HU treatment. After that, no PCNA-reactive cells were observed until 25 h after agent administration. After that time, the density of this parameter increased (Fig. 4). Similar results were obtained when the coronal plates were analyzed.

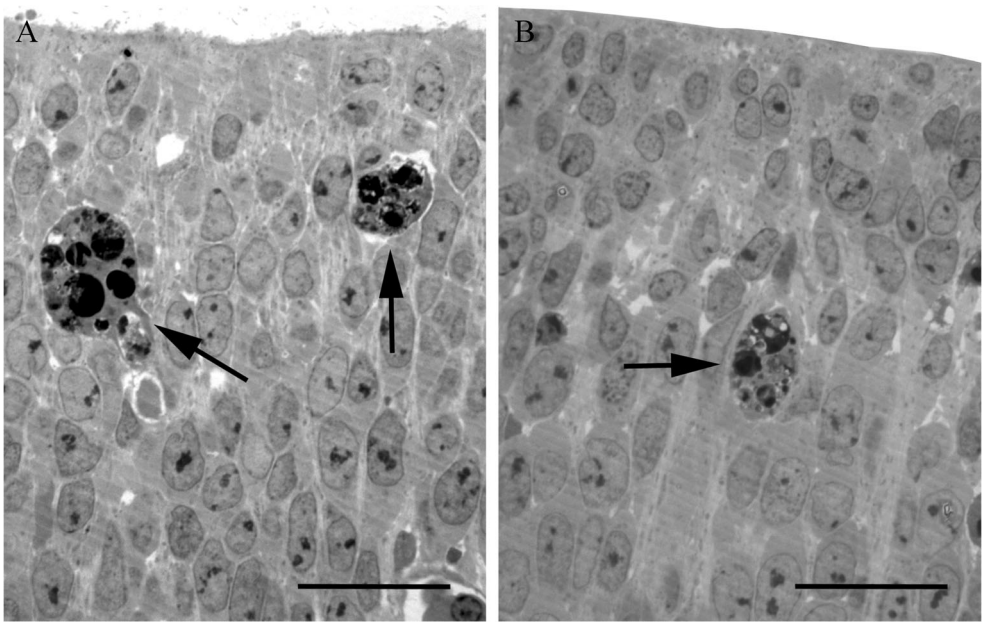

Fig. 7 Thin (0.6 μm) plastic sections from cerebellar neuroepithelia of rats exposed to HU at embryonic day 14 and killed 15 h later. **a**, **b** Reveal the striking difference between normal and apoptotic cells. Healthy cells present a homogeneous lightly stained nucleoplasm contained within an intact nuclear membrane. The apoptotic profiles (*black arrows*) have dark spherical balls randomly distributed within the cell. *Scale bar* 20 μm

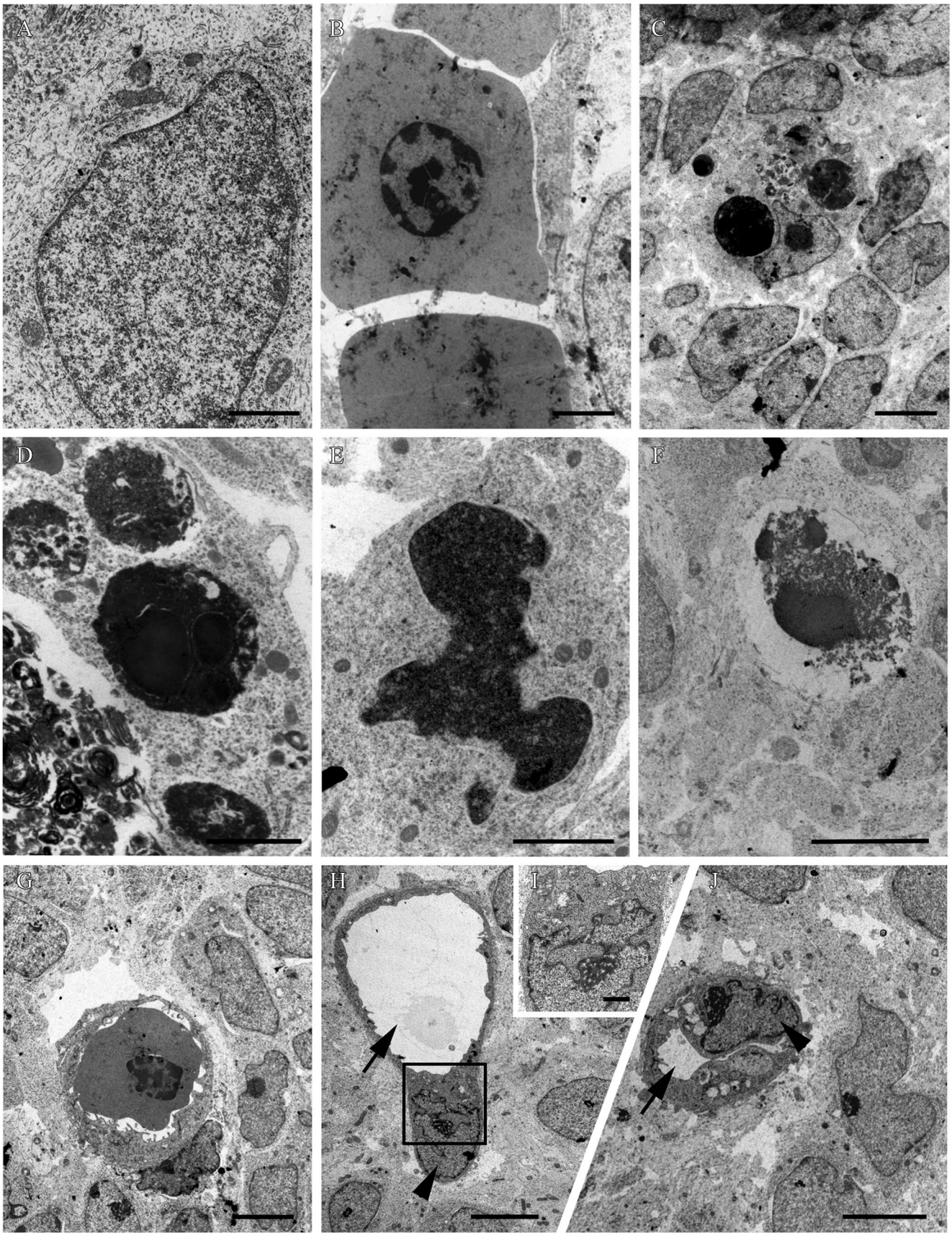
A
B
C
D
E
F
G
H
I
J

◀ **Fig. 8** Electron micrographs of healthy (**a**) and apoptotic cells (**b**–**j**) in the cerebellar neuroepithelium of rats exposed to hydroxyurea and sacrificed 20 h following drug administration. **b** An early stage of apoptosis showing conspicuous clumps of nuclear chromatin at the margin of the nucleus. **c**, **d** A late apoptotic stage showing typical clusters of apoptotic bodies. They present round and very electron-dense nuclear fragments. **e** An atypical example of a chromatin mass not perfectly spherical. **f** Breakup of an apoptotic body and release of its contents into the cytoplasm. **g** An apoptotic cell being engulfed by a glial cell. **h**–**j** Neuroepithelial cells exhibiting the cytoplasm with a large vacuole (*arrows*) and intact nuclei (*arrowhead*). The area in the *rectangle* in H is shown at higher magnification in **i**. **i** High-magnification detail showing degenerating mitochondria. *Scale bar*: 1 μm (**a**, **i**), 2 μm (**b**, **d**, **e**), 5 μm (**c**, **f**–**h**, **j**)

From these results, our basic information is that the administration of HU induces deleterious effects on the cerebellar neuroepithelium.

Experiment 2

There are evidences revealing that HU leads to the activation of apoptotic cellular events in the mouse fetal telencephalon (Woo et al. 2003, 2006) and in the cerebellar external granular layer of rats sacrificed in the early postnatal life (Martí et al. 2017). Also, previous data from our laboratory indicated that when HU is administered in the early embryonic period, the number of PCs and DCN neurons decreases and both the neurogenetic timetables and the neurogenetic gradients of these macroneurons are altered (Martí et al. 2016). In the light of the above, we used TUNEL reaction and transmission electron microscopy to characterize the type of cell death induced by HU exposure in the cerebellar neuroepithelium.

Figure 5 illustrates the variation in the density of TUNEL-positive cells in the cerebellar neuroepithelium of rats exposed to HU at E14. TUNEL-reactive cells were intensely and selectively labeled among hematoxylin-stained cells. Dying cells were distributed throughout the cerebellar neuroepithelium, with no evidence of preferential location.

With regard to the mediolateral axis, data of the density of TUNEL-positive cells, in addition to the statistical analysis of the former parameter, are depicted in Fig. 6. Our results revealed that, in all of the studied sagittal plates (1 to 4) and time-windows (from E13 to E15), TUNEL-stained nuclei started to appear in the cerebellar neuroepithelium 5 h after HU injection, and their values increased from 10 to 30 h. At 35 h, the density of TUNEL-positive nuclei declined. Conversely, only a few TUNEL-positive cells were detected in animals injected with saline. Similar results were obtained when the coronal plates were analyzed.

Apoptosis presents a series of ultrastructural features (Dikranian et al. 2001; Elmore 2007; Lossi and Gambino 2008). To confirm morphological features of cell death, light and electron microscopy were used to study all plates (sagittal and coronal) and time-windows (E13, E14, and E15). Our results showed that, when plastic thin sections were examined with light microscopy, the cerebellar neuroepithelium from rats administered with saline comprised several layers of small, darkly stained and densely packed cells, most of which were round-like in shape. Mitotic cells were present. In rats treated with HU, on the other hand, an important number of degenerating cell profiles was observed in all of the studied time-windows. Microscopic analysis revealed prominent alterations consistent with an apoptotic process, including the presence of spherical chromatin balls (Fig. 7).

In a subsequent study, we examined large numbers of neuroepithelial cells treated with HU using an electron microscope. The existence of cell death by apoptosis was confirmed by ultrastructural analysis. The presence of neuroblasts undergoing apoptotic degeneration was a very consistent finding from 5 to 35 h after the onset of HU exposure. The first detectable ultrastructural change was the condensation of the chromatin and its segregation against the inner nuclear envelope. The masses of compact chromatin display a high electron density (Fig. 8b). These initial changes were followed by the presence of spherical apoptotic bodies containing condensed dark chromatin masses. This occurs while the nuclear envelope remains intact and the cytoplasmic organelles are relatively unaltered (Fig. 8c, d). Sometimes, chromatin masses were not spherical (Fig. 8e) or they were broken and their contents extruded into the cytoplasm (Fig. 8f). Other ultrastructural changes included apoptotic cells engulfed by surrounding phagocytic cells (Fig. 8g). On the contrary, only a few cells displaying apoptotic morphology were detected in the saline-treated rats.

The current ultrastructural study also revealed that, in all of the time points studied, some neuroepithelial cells exposed to HU presented, in a well-preserved surrounding tissue, a vacuolated cytoplasm, deteriorated organelles, and a recognizable cell nucleus (Fig. 8h–j). This unusual cell death was not found in saline-administered animals. Our observations also revealed that these cells coexisted with apoptotic profiles, but they were not overlapping in the same neuroblast.

To summarize, our current observations indicate that the morphological features of apoptosis and unusual cell death appeared in the cerebellar neuroepithelium after HU exposition.

Discussion

The present study demonstrates that a single administration of HU in utero induces substantial depletion of cerebellar neuroepithelial cells, suggesting that the prenatal cerebellum is highly vulnerable to HU exposure. Our data reveal that E13, E14, and E15 are stages of high susceptibility to environmental insults.

The action of HU largely depends on its effect on nucleic acid synthesis in dividing cells. Hydroxycarbamide affects the S-phase by inhibiting ribonucleoside reductase, an important enzyme for DNA synthesis (Doi 2011). The depletion of DNA precursors due to HU causes the arrest of the replication fork, leading to cell death (Green and Barral 2014). It has been suggested that the activation of p38 mitogen-activated protein kinase pathways plays a role in mediating the specific malformations observed after HU exposure (Banh and Hales 2013).

Several studies have indicated that HU may have minimal or no effects on the developing human fetus (Thauvin-Robinet et al. 2001; Ballas et al. 2009). Despite that, the Center for the Evaluation of Risks to Human Reproduction is concerned that HU may increase the risk for congenital anomalies or growth abnormalities in fetuses after exposure of pregnant women (Lanzkron et al., 2008; Strouse et al. 2008). Moreover, previous research has indicated that the administration of the teratogenic agent HU to embryo rodents produces defects in the central nervous system and the skeleton (Woo et al. 2003, 2004; Schlisser and Hales 2013). The aim of the current study was to evaluate more accurately the consequences of HU exposure in the prenatal life.

As the cerebellar neuroepithelial cells have a high proliferating activity, they are susceptible to HU treatment. In our experimental model, mitotic figures and PCNA-reactive cells were found 25 h after HU treatment, suggesting that some neuroepithelial cells have the potential to resume proliferative activity after being injured. Despite that, the balance between proliferation and cell death is disturbed. The degree of damage induced by HU and the extent of the subsequent repair process would dramatically influence the level of abnormalities in the cerebellum. As PCs and DCN neurons are the first cells emerging from the cerebellar neuroepithelium (Altman and Bayer 1997; Wullimann et al. 2011; Leto et al. 2012) and the times of HU exposure (from E13 to E15) correspond with the period of neurogenesis of these macroneurons (Altman and Bayer 1997; Martí et al. 2015, 2016), we suggest that several PCs and deep neurons were never generated. In line with these results, previous data from our laboratory had reported that PCs were depleted following prenatal exposure to HU when assessed at 90 days of age (Martí et al. 2016). As the cerebellum is involved in sensorimotor operations, cognitive tasks, and affective processes (Samson and Claassen 2017), alterations in this region of the central nervous system might be involved in psychiatric and developmental disorders.

The results of our light and electron microscopy study show that exposure of the prenatal rat cerebellum to HU induces an apoptotic reaction that deletes large numbers of cell precursors. Pyknotic cells of those fetuses from dams that were injected with HU were stained by the TUNEL method, indicating that the neuroepithelial cells died by apoptosis. At all of the time-windows studied (from E13 to E15), degenerating cells in the cerebellar neuroepithelium displayed DNA fragmentation. Apoptotic profiles were seen along the anteroposterior and mediolateral axes.

To confirm that HU induces apoptosis in the cerebellar neuroepithelium, ultrastructural studies were performed. With electron microscopy, it was possible to see images of apoptosis, such as chromatin condensation, nuclear fragmentation, and presence of apoptotic bodies. Similar images have been found after HU injection in the mouse fetal telencephalon (Woo et al. 2003, 2006) as well as in the cerebellar external granular layer (Martí et al. 2017). Extensive apoptosis in the central nervous system has also been observed in response to prenatal treatments such as administration of 5-azacytidine (Hossain et al. 1995; Ueno et al. 2002), NMDA antagonists (Ikonomidou et al. 1999), ethanol (Ikonomidou et al. 2000), isoflurane (Creeley et al., 2014), and γ-radiation (Borovitskaya et al. 1996).

Despite the fact that the TUNEL method is widely used to detect apoptotic DNA fragmentation in tissue samples, its specificity has been questioned. This is because the TUNEL assay reaction can also detect necrotic cells (Charriaut-Marlangue and Ben-Ari 1995; Baima and Sticherling 2002). Our electron micrographs demonstrate that the prenatal administration of HU also produces an unusual cell death in the cerebellar neuroepithelium, which coexists with apoptotic profiles. We do not know the nature of this cell death. This is presumably due to the diversity of ultrastructural patterns that death assumes in cells under different extrinsic stresses (Castagna et al. 2016). For example, it has been reported in a model of neonatal ischemia that apoptotic cortical cells occur together with dying cells presenting morphological characteristics of necrosis, such as large cytoplasmic vacuoles, disappearance of organelles, and nuclear condensation (Wei et al., 2006; Parmenter et al. 2012). In addition to this, cells with ultrastructural features (vacuolated cytoplasm and intact nucleus) not fitting into the descriptions of apoptosis or autophagy have been reported in the cerebellar external granular layer of wild-type and *reeler* mice (Castagna et al. 2016). To our knowledge, this is the first report indicating that the administration of HU in the embryonic life triggers two types of cerebellar damage, one having apoptotic characteristics and the other presenting features that do not meet criteria for apoptosis. From these findings, the fetal cerebellum seems to be highly sensitive to chemicals and easily develops cell death. Our results are transposable to other regions of the central nervous system and may be useful to determine the impact of a particular treatment in living tissues.

Conclusions

We have demonstrated that rat cerebellar neuroepithelium is highly vulnerable to HU treatment. Our study provides a clue

for investigating the mechanisms of this agent-induced toxicity in the prenatal development of the central nervous system. Considering the magnitude to which cell death contributes to the effects of HU exposure, our results call for the necessity to better understand and define the administration of this agent to gestating women. This is because alterations of the cerebellar development have been associated with many pathological conditions, such as autism, neuropsychiatric disorders, and, intriguingly, type 1 diabetes mellitus (Allin 2016). Further studies with laboratory animals receiving HU treatment during the early prenatal life are required before this agent can be promoted as safe for human fetus.

Acknowledgments The authors are very grateful to Drs. María del Carmen Santa-Cruz and José Pablo Hervás for providing the animals.

Compliance with Ethical Standards All experiments in this study were carried out in accordance with the requirements of the Committee for Institutional Animal Care and Use in the Universitat Autònoma de Barcelona (UAB).

Conflict of Interest The authors declare that they have no conflicts of interest.

References

Allin MP (2016) Novel insights from quantitative imaging of the developing cerebellum. Semin Fetal Neonatal Med 21(5):333–338

Altman J, Bayer SA (1985) Embryonic development of the rat cerebellum I. Delineation of the cerebellar primordium and early cell movements. J Comp Neurol 231:1–26

Altman J, Bayer SA (1995) Atlas of prenatal rat brain development. CRC Press Inc., Boca Raton

Altman J, Bayer SA (1997) Development of the cerebellar system: in relation to its evolution, structure and functions. CRC Press Inc., Boca Raton

Baima B, Sticherling M (2002) How specific in the TUNEL reaction? An account of a histochemical study on human skin. Am J Dermatopathol 24:130–134

Ballas SK, McCarthy WF, Guo N, DeCastro L, Bellevue R, Barton BA, Waclawiw MA, Multicenter Study of Hydroxyurea in Sickle Cell Anemia (2009) Exposure to hydroxyurea and pregnancy outcomes in patients with sickle cell anemia. J Natl Med Assoc 101(10):1046–1051

Banh S, Hales BF (2013) Hydroxyurea exposure triggers tissue-specific activation of p38 mitogen-activated protein kinase signaling and the DNA damage response in organogenesis-stage mouse embryos. Toxicol Sci 133(2):298–308

Borovitskaya AE, Evtushenko VI, Sabol SL (1996) Gamma-radiation-induced cell death in the fetal rat brain possesses molecular characterisitics of apoptosis and is associated with specific messenger RNA elevations. Mol Brain Res 35:19–30

Butts T, Green MJ, Wingate RJ (2014) Development of the cerebellum: simple steps to make a "little brain". Development 141:4031–4041

Castagna C, Merighi A, Lossi L (2016) Cell death and neurodegeneration in the postnatal development of cerebellar vermis in normal and Reeler mice. Ann Anat 207:76–90

Charriaut-Marlanque C, Ben-Ari Y (1995) A cautionary note on the use of the TUNEL stain to determine apoptosis. Neuroreport 7(1):61–64

Creeley CE, Dikranian KT, Dissen GA, Back SA, Olney JW, Brambrink AM (2014) Isoflurane-induced apoptosis of neurons and oligodendrocytes in the fetal rhesus macaque brain. Anesthesiology 120(3):626–638

Dikranian K, Ishimaru MJ, Tenkova T, Labruyere J, Qin YQ, Ikonomidou C, Olney JW (2001) Apoptosis in the *in vivo* mammalian forebrain. Neurobiol Dis 8:359–379

Doi K (2011) Mechanisms of neurotoxicity induced in the developing brain of mice and rats by DNA-damaging chemicals. J Toxicol Sci 36(6):695–712

Elmore S (2007) Apoptosis: a review of programmed cell death. Toxicol Pathol 35:495–516

Green NS, Barral S (2014) Emerging science of hydroxyurea therapy for pediatric sickle cell disease. Pediatr Res 75(1–2):196–204

Grimaldi P, Parras C, Guillemot F, Rossi F, Wassef M (2009) Origins and control of the differentiation of inhibitory interneurons and glia in the cerebellum. Dev Biol 328:422–433

Haines DE, Dietrichs E (2012) The cerebellum, structure and connections. Handb Clin Neurol 103:3–36

Hervás JP, Martí-Clúa J, Muñoz-García A, Santa-Cruz MC (2002) Proliferative activity in the cerebellar ext ernal granular layer evaluated by bromodeoxyuridine labeling. Biotech Histochem 77:27–35

Hossain MM, Nakayama H, Goto N (1995) Apoptosis in the central nervous system of developing mouse fetuses from 5-azacytidine-administered dams. Toxicol Pathol 23(3):367–372

Ikonomidou C, Bosch F, Miksa M, Vockler J, Bittigau P, Pohl D, Dikranian K, Tenkova T, Turski L, Olney JW (1999) Blockade of NMDA receptors and apoptotic neurodegeneration in the developing brain. Science 283:70–74

Ikonomidou C, Bittigau P, Ishimaru MJ, Wozniak DF, Koch C, Genz K, Price MT, Stefovska V, Hörster F, Tenkova T, Dikranian K, Olney JW (2000) Ethanol-induced apoptotic neurodegeneration and fetal alcohol syndrome. Science 287:1056–1060

Lanzkron S, Strouse JJ, Wilson R, Beach MC, Haywood C, Park H, Witkop C, Bass EB, Segal JB (2008) Systematic review: hydroxyurea for the treatment of adults with sickle cell disease. Ann Intern Med 148:939–955

Lebwohl M, Menter A, Koo J, Feldman SR (2004) Combination therapy to treat moderate to severe psoriasis. J Am Acad Dermatol 50(3):416–430

Leto K, Bartolini A, Yanagawa Y, Obata K, Magrassi L, Schilling K, Rossi F (2009) Laminar fate and phenotype specification of cerebellar GABAergic interneurons. J Neurosci 29(21):7079–7091

Leto K, Rolando C, Rossi F (2012) The genesis of cerebellar GABAergic neurons: fate potential and specification mechanisms. Front Neuroanat 6:6. doi:10.3389/fnana.2012.00006. eCollection

Leto K, Arancilo M, Becker EBE, Buffo A, Chiang C, Ding B, Dobyns WB, Dusart I, Haldipur P, Hatten ME, Hoshino M, Joyner AL, Kano M, Kilpatrick KJ, Koibuchi N, Marino S, Martínez S, Millen KJ, Millner TO, Miyata T, Parmigiani E, Schilling K, Sekerkova G, Sillitoe RV, Sotelo C, Uesaka N, Wefers A, Wingate RJT, Hawkes R (2016) Consensus paper: cerebellar development. Cerebellum 15:789–828

Lossi L, Gambino G (2008) Apoptosis of the cerebellar neurons. Histol Histopathol 23:367–380

Manto M (2012) Toxic agents causing cerebellar ataxias. Handb Clin Neurol 103:201–213

Martí J, Santa-Cruz MC, Serra R, Hervás JP (2015) Systematic differences in time of cerebellar-neuron origin derived from bromodeoxyuridine immunoperoxidase staining protocols and tritiated thymidine autoradiographic: a comparative study. Int J Dev Neurosci 47:216–228

Martí J, Santa-Cruz MC, Serra R, Hervás JP (2016) Hydroxyurea treatment and development of the rat cerebellum: effects on the neurogenetic profiles and settled patterns of Purkinje cells and deep cerebellar nuclei neurons. Neurotox Res 30(4):563–580

Martí J, Molina V, Santa-Cruz MC, Hervás JP (2017) Developmental injury to the cerebellar cortex following hydroxyurea treatment in early postnatal life: an immunohistochemical and electron microscopic study. Neurotox Res 31(2):187–203

Martínez S, Andreu A, Mecklenburg N, Echevarria D (2013) Cellular and molecular basis of cerebellar development. Front Neuroanat 7:18. doi:10.3389/fnana.2013.00018 eCollection 2013

Marzban H, Del Bigio MR, Alizadeh J, Ghavami S, Zachariah RM, Rastegar M (2015) Cellular commitment in the developing cerebellum. Front Cell Neurosci 8:450. doi:10.3389/fncel.2014.00450. eCollection

Navarra P, Preziosi P (1999) Hydroxyurea: new insights on an old drug. Crit Rev Oncol Hematol 29:249–255

Nevitt SJ, Jones AP, Howard J (2017) Hydroxyurea (hydroxycarbamide) for sickle cell disease. Cochrane Database Syst Rev 4:CD002202. doi:10.1002/14651858.CD002202.pub2

Pamenter ME, Perkins GA, McGinness AK, Gu XQ, Ellisman MH, Haddad GG (2012) Autophagy and apoptosis are differentially induced in neurons and astrocytes reated with an in vitro mimic of the ischemic penombra. PLoS One 7(12):e51469

Saban N, Bujak M (2009) Hydroxyurea and hydroxamic acid derivatives as antitumor drugs. Cancer Chemother Pharmacol 64:213–221

Sampson M, Archibong AE, Powell A, Strange B, Roberson S, Hills ER, Bourne P (2010) Perturbation of the developmental potential of preimplantation mouse embryos by hydroxyurea. Int J Environ Res Public Health 7:2033–2044

Samson M, Claassen DO (2017) Neurodegeneration and the cerebellum. Neurodegener Dis 17(4–5):155–165

Schilling K, Oberdick J, Rossi F, Baader SL (2008) Besides Purkinje cells and granule neurons: an appraisal of the cell biology of the interneurons of the cerebellar cortex. Histochem Cell Biol 130:601–615

Schlisser AE, Hales BF (2013) Deprenyl enhances the teratogenicity of hydroxyurea in organogenesis stage mouse embryos. Toxicol Sci 134:391–399

Shao J, Zhou B, Chu B, Yen Y (2006) Ribonucleotide reductase inhibitors and future drug design. Curr Cancer Drug Targets 6:409–431

Sillitoe RV, Joyner AL (2007) Morphology, molecular codes, and circuitry produce the three-dimensional complexity of the cerebellum. Annu Rev Cell Dev Biol 23:549–577

Strouse JJ, Lanzkron S, Beach MC, Haywood C, Park H, Witkop C, Wilson RF, Bass EB, Segal JB (2008) Hydroxyurea for sickle cell disease: a systematic review for efficacy and toxicity in children. Pediatrics 122(6):1332–1342

Thauvin-Robinet C, Maingueneau C, Robert E, Elefant E, Guy H, Caillot D, Casasnovas RO, Douvier S, Nivelon-Chevallier A (2001) Exposure to hydroxyurea during pregnancy: a case series. Leukemia 15(8):1309–1311

Tong KK, Ching Ma T, Kwan M (2015) BMP/Smad signaling and embryonic cerebellum development: stem cell specification and heterogeneity of anterior rhombic lip. Develop Growth Differ 57:121–134

Ueno M, Nakayama H, Kajikawa S, Katayama K, Suzuki K, Doi K (2002) Expression of ribosomal protein L4 (rpL4) during neurogenesis and 5-azacytidine (5AzC)-induced apoptotic process in the rat. Histol Histopathol 17(3):789–798

Ware RE, Despotovic JM, Mortier NA, Flanagan JM, He J, Smeltzer MP, Kimble AC, Aygun B, Wu S, Howard T, Sparreboom A (2011) Pharmacokinetics, pharmacodynamics, and pharmacogenetics of hydroxyurea treatment for children with sickle cell anemia. Blood 118:4985–4991

Wei L, Han BH, Li Y, Keogh K, Holtzman DMYSP (2006) Cell death mechanism and protective effect of erythropoietin after focal ischemia in the whisker-barrel cortex of neonatal rats. J Pharmacol Exp Ther 317(1):109–116

Woo GH, Katayama K, Jung JY, Uetsuka K, Bak EJ, Nakayama H, Doi K (2003) Hydroxyurea (HU)-induced apoptosis in the mouse fetal tissues. Histol Histopathol 18:387–392

Woo GH, Katayama K, Bak EJ, Ueno H, Tamauchi H, Uetsuka K, Nakayama H, Doi K (2004) Effects of prenatal hydroxyurea-treatment on mouse offspring. Exp Toxicol Pathol 56(1–2):1–7

Woo GH, Bak E-J, Nakayama H, Doi K (2005) Hydroxyurea (HU)-induced apoptosis in the mouse fetal lung. Exp Mol Pathol 79:59–67

Woo GH, Bak EJ, Katayama K, Doi K (2006) Molecular mechanisms of hydroxyurea (HU)-induced apoptosis in the mouse fetal brain. Neurotocol Teratol 28:125–134

Wullimann MF, Mueller T, Distel M, Babaryka A, Grothe B, Köster RW (2011) The long adventurous journey of rhombic lip in jawed vertebrates: a comparative developmental analysis. Front Neuroanat 5:27. doi:10.3389/fnana.2011.00027. eCollection

Yaguchi Y, Yu T, Ahmed MU, Berry M, Mason I, Basson MA (2009) Fibroblast growth factor (FGF) gene expression in the developing cerebellum suggests multiple roles for FGF signaling during cerebellar morphogenesis and development. Dev Dyn 238(8):2058–2072

Zala C, Rouleau D, Montaner JS (2000) Role of hydroxyurea in treatment of disease due to human immunodeficiency virus infection. Clin Infect Dis 30:S143–S150